Gripping in anthropomorphic robotics

A. Chesnot, N. Jensen, M. Seiffert, A. Hernandez, M. Zarea

Department of Materials and Production, Aalborg University
Fibigerstraede 16, DK-9220 Aalborg East, Denmark
Email: {achesn21, njens21, mzarea20, mseiff22, aherna21}@student.aau.dk,
Web page: http://www.mechman.mp.aau.dk/

Abstract
We introduce a data-driven and simulation-based approach for design of versatile, anthropomorphic grippers. An analysis of Non Invasive Adaptive Prosthetics (Ninapro) database is made to obtain kinematic simplifications of the human hand based on the record of multiple grasping techniques. Subsequently, a mechanical solution has been developed based on the post-processing of this experimental data resulting in a compact cable-driven system. The resulting gripper is then evaluated to determine its ability to perform several grasps of different objects.

Keywords: Anthropomorphic, Robotics, Hand, Ninapro database, Grasping technique

1. Introduction

There has been a growing interest in robotic hand development in the recent decades. In most gripping applications, the gripper is only designed to fit exactly one object. This process is not efficient because the grippers are not sufficiently versatile. Most industrial grippers have been limited to specific purpose grippers that are inadequate when dealing with objects of different sizes and shapes [1]. To achieve more versatility, many anthropomorphic robotic hands have been developed using some of the bio-mechanical advantages and techniques of the human hand [2]. A dexterous robotic hand design has certain properties that makes it desirable for industry. However, robotic hand dexterity can be severely compromised by an ineffective actuation, transmission, and design. Due to recent advances in robotic actuation systems, multiple under-actuated hands have been created [3], [4], [5], [6].

To create an anthropomorphic under-actuated robotic gripper, the human hand bio-mechanics have to be thoroughly researched. Moreover, grasping techniques are implemented and tested in a mechanical solution. This is done by means of static and kinematic analyses, where the model is able to perform several grasps to prove its dexterity and is under-actuated by statistical means of analysing experimental grasp data.

2. State-of-the-art

Industrial robots are often used in applications beyond the normal ability of conventional manpower. From millimeter-level precision to a highly repetitive grabbing procedure. Industrial grippers are typically sized and intended to do tasks that humans would struggle at, due to either physical or temporal constrains. Industrial grippers are fitted to purposefully grasp an object, thus their functionality is highly influenced by the type of grasping it applies on a object.

For industrial robotic grippers, dexterity has always been a challenging quality to achieve. Almost always, a compromise between high flexibility and grabbing force has to be made. The bio-mechanics of the human hand are the starting point for most attempts to improve flexibility. To that end, a classification of the different actuators regarding dexterous robotic hands will be discussed.

2.1 Actuation systems in anthropomorphic robotics

In the literature, three different types of actuators can be found: Motor-driven systems, where motors act as actuators producing the movements of the joints [3], Tendon-driven systems, where the actuators are placed in the forearm and the driving force is transmitted via tendons [7], and Linkage-driven systems where motors are directly placed on joints which result in a bulky and rigid system [8].

As a result of the preceding study, it can be concluded that, when designing a dexterous anthropomorphic robotic hand, the selection of the type of actuation is a critical factor in the design process. These robotic grippers take into account the environment and the grasping needs for the task required.

2.2 Grasping techniques

Stability in the human hand can be achieved by either a precision or a power grasp. Grasping an object depends on the purpose, the dimensions of the grasping hand or tool and the object's dimensions. This section categorizes the grasps based on the anatomical differences.

Power grasp

Power grasp utilize the hand's fingers to form one jaw clamp with the palm as the other jaw. The fingers flex depending on the dimensions of a certain object and are inclined towards the palm. The thumb pulp surface is used in this grasp type. In Fig. 1, opening a tight lid usually requires a power grasp to loosen the lid.

Precision grasp

Precision grasp utilizes the fingertips of the fingers and that of the opposing thumb to clamp an object. The posture of the thumb ensures that the sensory surfaces are deployed to their fullest allowing delicate adjustments of position and precise manipulations. In Fig. 1, as the lid is now loosened, the a hand switches to precision grasp to unscrew the lid easier.

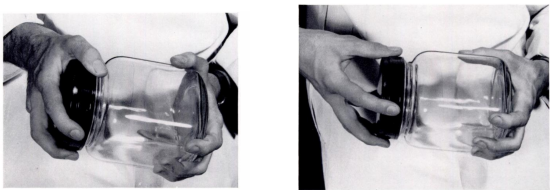

Fig. 1 Different types of grasp (left: Power grasp, right: precise grasp) [9].

3. Data analysis

A comprehensive analysis of the human hand is performed to understand which elements of the hand are crucial for grasping various objects. The scope is to derive design simplifications from this gained knowledge which are then used for the robotic gripper. Also, lower down the complexity of the human hand while maintaining its high dexterity.

This analysis is a prerequisite for the design of the robotic gripper. The focus is only on the main objectives of this project to prevent over designing of the robotic gripper.

For the analysis of the kinematics of the human hand, the Ninapro database 9 is used, a publicly available database that contains extensive data on the motion of the human hand during the execution of various tasks [10]. The right hand kinematics were measured with the CyberGlove II, a motion capturing data glove that measures the joint-angles with high-resolution resistive flex and bend sensors [11]. The data have been calibrated [10]. The recorded joint angles are displayed in Fig. 2.

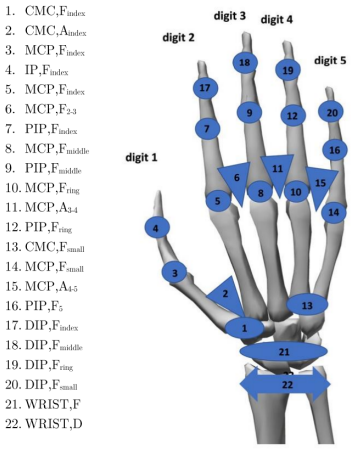

Fig. 2 List of recorded anatomical angles. Adapted from [10].

3.1 Data preprocessing

For the purpose of this project, the data are preprocessed. The data contain 40 hand movements that are divided in exercise sets B and C of 77 subjects in total [12]. For each subject, the data are stored in two separate Matlab matrix files, containing all the calibrated, continuously recorded joint angles of the exercise sets B and C [10]. The first step is to separate the data to evaluate each exercise separately.

Separation of exercises

All of the 22 joint angles are plotted over the sampling time (shown in Fig. 3 of subject 1, exercise set C [10]) to visualize the start and ending of each exercise. A python script is written to separate and save the exercises for all subjects for further investigation.

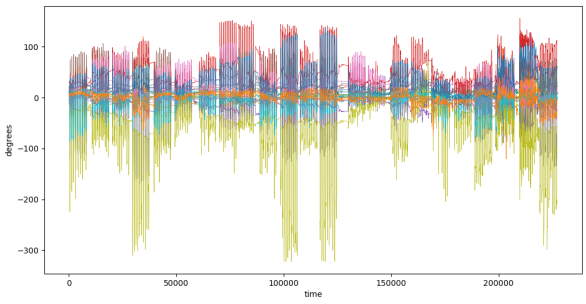

Fig. 3 Data of the 22 joints for all exercises.

Fig. 4 shows the extracted first exercise of the set of exercises C, resulting in a clear visualisation of all the ten repetitions.

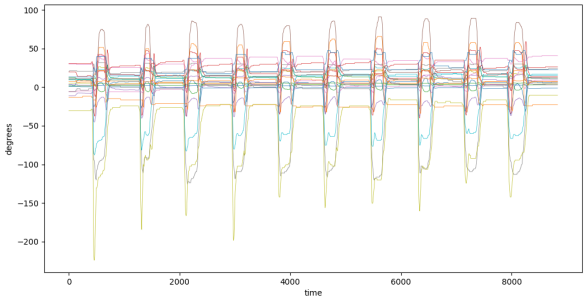

Fig. 4 Data for 22 joints for one exercise.

Compiling of mean movement

In the protocol of the Ninapro database 9 it is stated that many factors may affect the signal from the sensors during the recording of the data. These factors include fatigue of the the subjects during the performance of the repetitions, the acquisition setup, noise problems or slipping of the glove during the exercises [10]. Especially for subjects with smaller hands the glove could have a loose fit resulting in an imprecise sensor recording. In fact, that was a major problem for the sensors positioned to measure the distal interphalangeal (DIP) joint angles, resulting in unexpected peaks in the recordings. In addition the recordings show an extension of the joint angles when flexion is expected, which is interpreted as a malfunction in the calibration process.

To counteract these factors a mean movement is introduced. All of the ten repetitions for each exercise are processed into one mean movement. Small variations in repeatedly grasping the same object are converted to one smooth movement which provides the average of all repetitions for more precise evaluation. In this way outliers and unexpected peaks are smoothed out. A python file is written to compile the mean movement from all the repetition of each exercise of each subject. This is done by defining a start and end point for each exercise to then adding all repetitions up and divide it by the number of repetitions.

In Fig. 5 the recorded angles of all 22 joints are plotted for one repetition before processing. Fig. 6 shows the mean movement of the 22 joints after the processing. A more continuous movement of the angles is obtained when approaching and releasing the grasp. While the grasp is executed, each joint angle shows a steady behaviour at which the grasp is evaluated (red line in Fig. 6). Peaks that are caused by noise of the sensor or deviation caused by fatigue of the subject are counteracted.

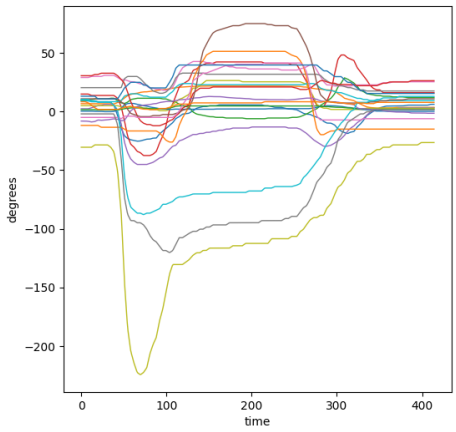

Fig. 5 Movement of the 22 joint angles performing exercise one of exercise set C [10] - before processing.

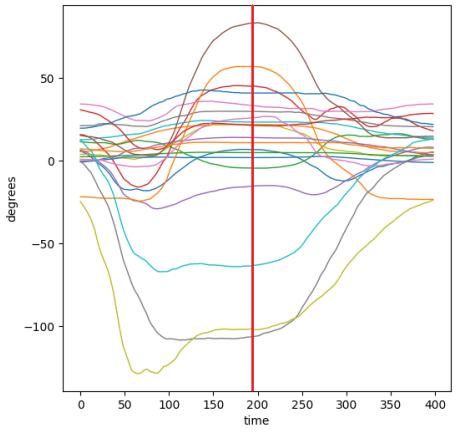

Fig. 6 Movement of the 22 joint angles performing exercise one of exercise set C [10] - after processing.

To confirm that the outcome of this preprocessing step is reasonable, the joint angle data of the compiled mean movement is inserted into the

complex hand model of the AnyBody Modeling System™ (AMS) which is displayed in Fig. 7.

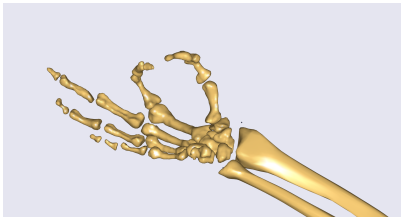

Fig. 7 Confirmation of the data in Anybody modeling system.

3.2 Investigation of the free moving hand

To confirm the dependency of the DIP and the proximal interphalangeal (PIP) joints, exercises B from the Ninapro are selected [10]. In this exercise the subject performs a task containing a flexion of the fingers to a fist. In this way the kinematics of the segments of the human hand can be studied without being counteracted by an object.

For ten subjects, the preprocessed data of exercise six that contains the mean movement of the ten repetitions is used for this investigation. To observe patterns of covariation the joint angles of the index finger are plotted against each other. In Fig. 8 the corresponding correlation coefficients are shown.

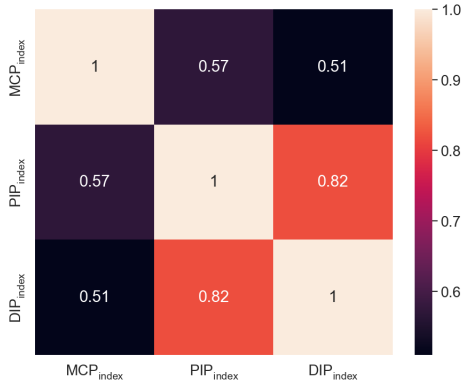

Fig. 8 Correlation coefficients of the joints in the index finger.

3.3 Examination of grasping various objects

Kinematic relations of the segments are examined when power and precision grasps are performed. Therefore exercise set C is evaluated containing power and precision grasps of various objects.

Range-of-motion

The range-of-motion (ROM) of all the joints are plotted in Fig. 9 when performing the precision and power grasps.

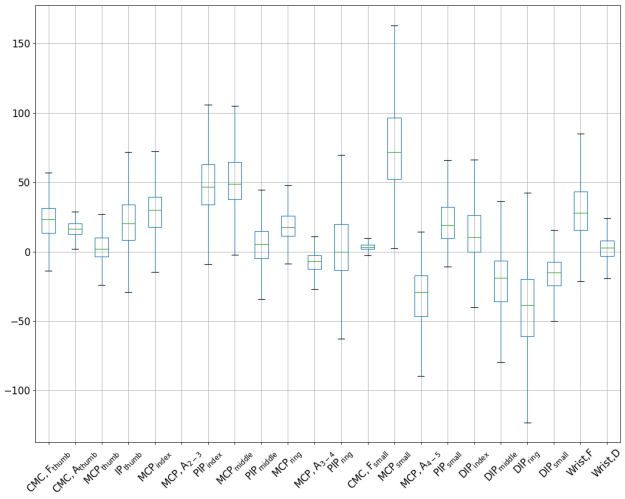

Fig. 9 ROM of the joints in the human hand while performing grasping exercises from the set of exercises C.

Patterns of covariation

A snapshot of the values of all the angles is taken in the middle of the phase when the grasp is performed. This is done for all the exercises of the set of exercises C for ten subjects [10]. To visualize patterns of covariation in the kinematics of the segments, all of the joint angles are plotted against each other for all the data. In addition, the corresponding correlation coefficients are plotted in a correlation matrix where a small section is shown in Fig. 10 for the metacarpal phalangeal (MCP) joints. In addition, the corresponding patterns of covariation are plotted in Fig. 11.

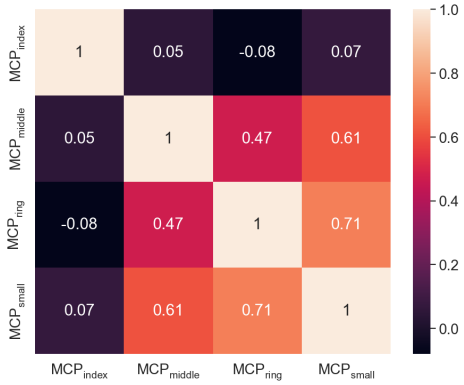

Fig. 10 Correlation coefficients of the MCP joints in set of exercises C.

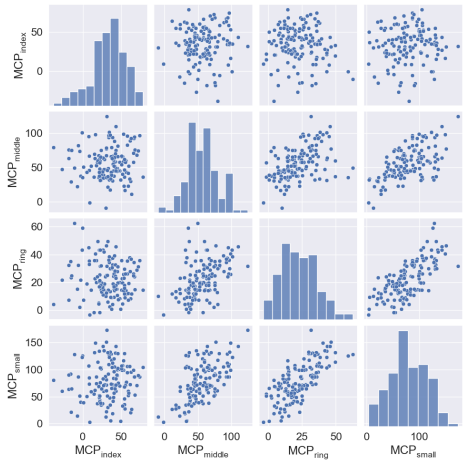

Fig. 11 Patterns of covariation of the MCP joints in set of exercises C.

3.4 Results and discussion

The results in the data analysis are derived to design simplifications that are adopted in the design process of the mechanical gripper.

Reduce the actuation / coupling of adjusted joints

Dependent behaviour can be observed in the data of the DIP and PIP joints while closing the hand. Fig. 8 shows a high correlation coefficient of 0.82 for the DIP and PIP joints of the index finger. Additionally, the correlation between the MCP and PIP joints and between the MCP and DIP joints is much lower. This dependency in the human hand can be derived to design simplifications:

- The DIP and PIP joints can be driven by one actuator when a linkage is created to move these two joints dependently to each other.

To obtain the dependency-factor that is implemented in the design process of the mechanical hand, the curve of each subject is linearly regressed and the mean value is calculated from all the subjects .

$$\frac{\Delta\phi_{DIP}}{\Delta\phi_{PIP}} \approx 0.57 \tag{1}$$

Since the sensor data of the DIP joints of the other fingers show unexpected results, they are excluded and the dependency-factor is used for all the fingers.

Another highly dependent pair of joint angles are found to be the MCP joints of two adjacent fingers. Fig. 11 shows the coefficients of correlation of the MCP joints while performing the various grips.

A high correlation factor of 0.71 indicates a positive correlation between the MCP joints of the little and ring fingers. A smaller correlation factor between the MCP joints between the ring and middle fingers indicates a less weighted correlation. Between the MCP joint of the index finger and the others no correlation was observed. This is interpreted as a result that the index finger is used separately from the other fingers in several exercises, especially to perform precision grasps [10].

Similar results are found for the PIP joints of the fingers. The PIP joints of the adjacent little and ring fingers show the highest correlation factor of 0.7, while the PIP joints of the index finger show a significantly lower correlation to the PIP joints of the other fingers.

The findings are interpreted in the following simplification for the design process:

- The small and ring fingers show a high positive correlation of each PIP joint and MCP joint, therefore an actuation method can be used to actuate these two fingers in a similar manner. Since the correlation is not truly linear, the actuation method allows small deviations.
- Since in the index finger, both PIP and DIP joints show low or no correlation to the adjacent fingers it should be actuated independently. The analysis of the data indicates that the index finger is especially important for several precision grasps, simplifications should therefore be avoided.

Removal of joints

In Fig. 9 it is observed that for some angles the ROM is comparatively small while performing grasps. This is the case for the carpometacarpal (CMC) joint of the thumb that is responsible for abduction. Another joint is the CMC, F_{small} which also shows a very small ROM in both power and precision grasps. Lastly, the MCP, A_{3-4} joint that is responsible for the abduction of the middle and ring fingers shows little ROM while the MCP, A_{4-5} joint shows a non-negligible greater ROM. This is interpreted as in many exercises the little finger needs to greatly abduct to enlarge the hand to grasp and surround larger objects. As a result, the following simplifications can be derived:

- The CMC joint of the thumb can be reduced and

replaced by a fixed angle. This is indeed a good simplification since for most of the precision and power grasps, the thumb is positioned at the opposite side to surround the grasped object and create a counter force.
- The CMC, F_{small} joint that is located in the palm can be removed since it shows very little ROM.
- The small ROM of the MCP, A_{3-4} joint indicates the removal of this joint. A small static angle should be chosen as seen in Fig. 9.
- The MCP, A_{2-3} joint was excluded from the database due to strong noise problems. However to further simplify the model this joint is removed. This simplification is proved in the later simulation phase.
- The MCP, A_{4-5} joint shows a greater ROM. Therefore, removing this joint may have a significant impact on the whole design. Thus, to ensure that the system can still achieve the described enlargement, appropriate adjustments must be made when removing this joint.

Adjustment of joints

In the previous design simplification, it is stated that the ROM of the MCP, A_{4-5} joint is relatively big. When removing this joint to simplify the model, the abduction angle of the little finger relatively to the adjacent fingers can be set to a larger, fixed angle. In this way it is still possible to surround bigger objects and provide a better stability of the grasp.

In addition, the data show unexpected results for this joint. In Fig. 9 the mean value is stated to be negative even though the abduction of this joint is defined as positive. Thus, the MCP, A_{4-5} joint can be removed and the abduction angle should be set to a higher value to provide better stability of the grasped object.

Restrict the range-of-motion

When applying power and precision grasps it can be observed in the data that the joints are performing a ROM that is smaller than the actual limitations in the human hand. The finger joints of the human hand (MCP, DIP) are not limited to flexion only but also allow extension. The results from the data of the ROM shown in Fig. 9 give a strict positive ROM for the MCP joints of all the fingers. These joints can therefore be limited to flexion movements.

In the data the PIP joints also show a ROM that is limited to flexion. The PIP joint of the ring finger however shows also signs of extension. The ROM for all DIP joints shows extension except for the index finger. This is interpreted as a malfunction in either recording or calibration of the data since these angles should vary while the flexion of the fingers is occurring. Summarized, these findings leads to the following design simplifications:

- The ROM of the finger joints MCP, PIP, DIP joints can be limited to flexion.

The PIP joint of the ring finger also shows an extension movement, but the simulations reveal that limitation to flexion is acceptable for this finger as well.

4. Design of the robotic gripper

From the simplifications stated in the *Data analysis* chapter, a mechanical solution is designed. It is divided into four main modules, namely precision and power fingers, thumb and the palm.

4.1 Divide into realizable modules

The first module comprises the precision fingers, which act as the index and middle fingers. Based on the results of the data analysis, a dependency is created between the PIP and DIP joints.

The second module covers the power fingers which correspond to the ring and little fingers of the human hand. These are mostly used for power grasps and thus, the design's complexity is reduced. A dependency is also present between the DIP and MCP joints.

The thumb composes the third module. The CMC joint and the abduction movement of the MCP joint are removed. However, the flexion of the MCP joint remains.

The fourth module is the palm and the modules mentioned before are fixed to it. The fixation of the different modules are oriented with an angle to reproduce the abduction position.

4.2 Design of the solution principles

To move the segments of the fingers, the joints are actuated by a cable mechanism, which converts pulling force into an articulation of the joints. An important factor when actuating the joints is that the lever arm remains constant for any given angle to prevent singular positions. It also provides a constant

torque. To avoid that the lever arm varies during the rotation of the joint, the actuation cable is guided around the joint on a wheel with a constant diameter.

To ensure the rotational dependency and a constant torque in the joints, a cable as shown in Fig. 12 connects the outer and middle segments of each finger. The difference of radius of the two wheels leads to the rotation ratio $\Delta\Phi_{DIP}/\Delta\Phi_{PIP} = 0.6$.

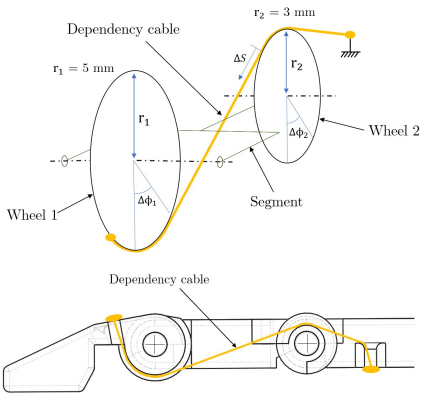

Fig. 12 Dependency between the 2 wheels.

The initial position of the robotic gripper is when all the fingers are in the same plane. The extension movement of the fingers is carried out by springs. Inspired by the anatomy of the human hand, a cable is hooked to the last joint (see Fig. 13) and passes over the finger up to the palm where the spring is localized. To ensure that the cable maintains its position, a groove guides the cable.

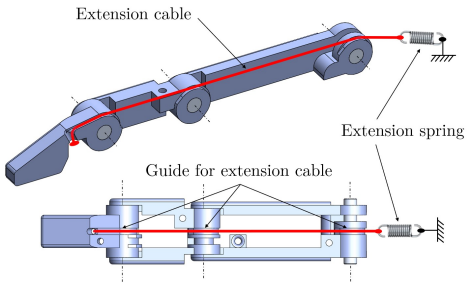

Fig. 13 Extension cable system of the precision finger.

4.3 Assembly of each modules

The precision fingers, as shown in Fig. 14, are made up of three segments connected together by revolute joints. As described in the *Data analysis* section, the movement of the DIP and PIP joints are dependent on each other. However, the movement of the MCP joint is independent.

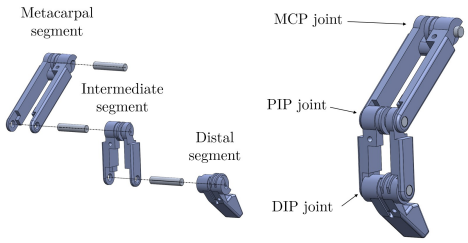

Fig. 14 Precision finger detailed view.

The power finger is made up of two segments as shown in Fig. 15. The segments are connected by a revolute joint and actuated by one cable. Another cable is responsible for the dependency between the MCP and PIP joints.

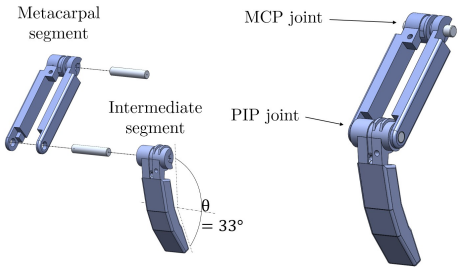

Fig. 15 Power finger detailed view.

Similarly, the thumb is made up of two segments but there is no dependency between the joints as shown in Fig. 16.

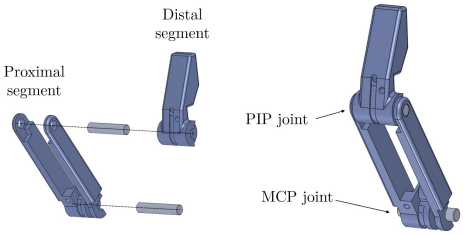

Fig. 16 Thumb detailed view.

The palm is used to combine all previous modules. All the cables converge to the palm and are guided to the forearm, where the actuators are assumed to be located. Guides and a cover ensure that the pulling cables remains in position when the grasp is performed. The extension cables pulled by the springs are placed on the other side of the palm.

5. AnyBody Simulation

A model is constructed to evaluate the solution's performance to determine appropriate components. Cables, springs, and motors have to be designed

to fulfill the system's requirements as well as the kinematics associated with the grasping techniques. For such a task, AnyBody Modeling System 7.3 (AMS) is used to perform static analyses of various grasps [13], [14].

5.1 Cables

Cables were designed to be wrapped around the different joints as shown previously. The material used is Nylon [15], which provides sufficient strength to resist the forces while the gripper is performing different grasps [16].

5.2 Springs

The springs localized on the outer side of the robotic gripper are assumed to be linear. Thus, the spring force is expressed through Hooke's law equation (Eq. 2).

$$F = -(k \cdot x) - L_0 \tag{2}$$

The springs must maintain the gripper on its initial position. Therefore, the springs must balance the gravity forces applied to the components. A springs-in-series model was considered and the stiffness of the global spring is then the sum of all the individual stiffness of each sub-spring.

5.3 Modelling of the grasps

The objects chosen to evaluate the gripper's performance are based on the work done by Jarque-Bou et al. [10]. They are common objects that the human hand can grasp. Using AMS, a static analysis of the two grasps is performed to determine the forces inside the cables that allow the gripper to hold the objects through the friction forces in the contact points.

Precision grasp

A pen is considered as the minimum volume object that can be handled by the robotic gripper. For this analysis, two contact points are defined, one at the tip of the thumb and the other at the tip of the middle finger (see Fig. 17).

Power grasp

A water bottle is considered as the maximum volume object that can be handled by the robotic gripper. Three contact points are defined, one at the tip of the thumb, one at the tip of the ring finger and another one on the first segment of the little finger (see Fig. 17).

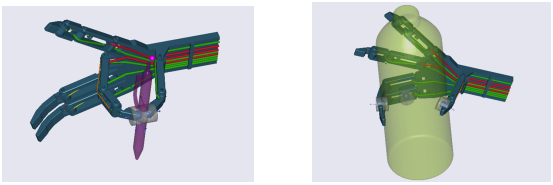

Fig. 17 Representation of the two grasps in AMS. (Left: precise grasp, right: power grasp).

No restriction is made on the sturdiness of the object, therefore it is assumed that the objects are sufficiently resistant to bear the normal forces of the contacts. Brorson et al. [17] estimated a mean normal pinch force of 60 N for a male person, which is assumed to be the normal force of the robotic gripper. The contact area is round to 4 mm^2, which results in a maximum contact strength of 15 MPa. Furthermore, a low static friction coefficient of 0.1 was used to guarantee that the final design is acceptable even with poor contact quality.

6. Results and Discussions

An overview of the final design of the robotic gripper is covered in this section.

6.1 Mechanical solution

The mass of the robotic gripper does not exceed 113g. The dimensions of each module are listed in Tab. I.

Tab. I Dimension for the different modules (mm).

	Length	Width	Height
Precision finger	100	20	12
Power finger	97	20	12
Thumb	82	18	10
Palm	131	96	27

The system has 12 revolute joints which results in eight DOFs. The ROM can be compared to that of the human hand. Due to the simplifications made in the 3 section, the robotic gripper does not possess abduction for the fingers and thumb. In addition, it can only close the digits in flexion. The extension is constrained to the initial position where all the fingers are in the same plane. However, there is no need for a larger extension since it is not used in the grasping techniques.

6.2 Dependency in the power fingers

The dependency found in Section 3 between the MCP and PIP joints of the power fingers is not

relevant for the grasp of the objects, especially if the value is too low to produce a contact point with the object. The power grasp of the bottle was used as a reference since this object defines the largest volume that the gripper should grasp. The ratio between the MCP joint angle over the PIP joint is shown in Eq. 3.

$$\frac{\Delta\Phi_{MCP}}{\Delta\Phi_{PIP}} \approx 0.357 \tag{3}$$

6.3 Springs

The inverse dynamic analysis of the robotic gripper from its initial position to the closing of all the fingers and thumb determined the Hooke's Law equation for the springs. The values of the pre-loads, the maximum elongation as well as the stiffness of the springs are shown in Tab. II.

Tab. II Stiffness and Pre-loads from the finger springs.

Finger	Stiffness(N/m)	Pre-load (N/m)	Elongation(cm)
Precise	-0.604	-0.8312	12.5
Power	-0.4735	-0.532	11
Thumb	-0.15	-0.32416	4.4

It should be noted that the residual forces of the motors were not taken into account. In addition, the joints are assumed to be ideal and the overall friction of the system has been neglected.

6.4 Cables

The material for the cables was chosen as Nylon with a tensile strength of 90 MPa for the analyses [16]. The robotic gripper was analyzed when holding a water bottle of 1.5 kg for the power grasp and a pen of 20g and 200g for the precision grasp. The results are shown in Tab. III. The cable that actuates the PIP joint is called cable no. 1 while the cable that actuates the MCP joint is called cable no. 2.

The cable no. 2 of the thumb is carrying all the load imposed on it in the power grasp. This cable experiences the highest pulling-force of the robotic gripper with a value of 241 N. On the other hand,

Tab. III Resulting forces in the cables for the different grasps (N).

		Index		Middle		Ring	Little	Thumb	
		1	2	1	2	1	1	1	2
Power		0.604	0.776	0.0896	0.115	57.4	168	4.78	241
Precise	20g	0.604	0.776	18.5	12	0.81	0.027	24	10.2
	200g	0.604	0.776	127	76.5	0.81	0.0227	167	0.85

the cable of the ring finger takes the lowest load with a force of 57 N for this grasp.

In the same way, the results for the precision grasp of a pen are shown in the second and third rows in Tab. III. Both grasps are identical except that the mass of the pen is increased from 20g to 200g in the second analysis. It can be seen that the load is not evenly distributed between the cables. Thus, the overall maximum force inside the cables is found in the power grasp of the bottle. Considering the strength of the Nylon and without any safety factor, a diameter of 1.85mm may be chosen for the cables.

6.5 Kinematic and grasping performance

To evaluate the ability of the robotic gripper to grasp different shapes, the simulation of the grasp of five common objects that are a ball, bottle, pen, cap bottle, and a disk is studied. As a result, the robotic gripper is able to perform these grasps as shown in Fig. 18, in particular with the dependencies implemented on the fingers. It should be noted that only the final posture is considered and no resulting forces were calculated.

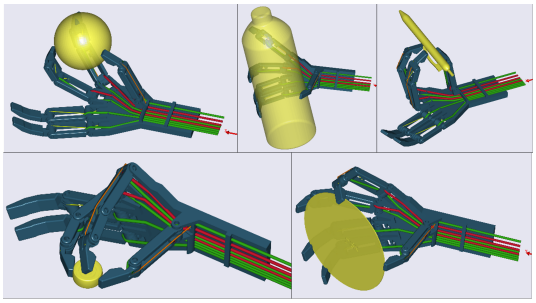

Fig. 18 Grasp of five common objects. (ball, bottle, pen, cap bottle, disk)

7. Conclusion

The design of a robotic gripper was developed based the analysis of the Ninapro database. The mechanical system has 12 joints, eight DOFs and can perform several grasps of different objects. Four main modules were created to meet the system's requirements while using the simplifications from the experimental data to reduce the complexity of the design. Most of these adjustments are either the removal of selected DOFs from the kinematic of the human hand or the creation of dependencies between joints' angles. It also uses a passive retraction method to move the hand back to its initial position. Finally, using AMS, it has been confirmed that the robotic gripper is able to perform motions that correspond to

the grasps of several objects. A further work could be the choice of the servomotors since the maximum involved forces on the cables have been determined. Moreover, the manufacturing of a prototype of the robotic gripper using 3D printing can be made to proceed to experimental testing of the solution. Besides, sensors should be included and a control system implemented to perform grasp using feedback information.

Acknowledgement
The authors of this work gratefully acknowledge Grundfos for sponsoring the 10th MechMan symposium.

References

[1] S. Cobos, M. Ferre, M. S. Uran, J. Ortego, and C. Pena, "Efficient human hand kinematics for manipulation tasks," in 2008 IEEE/RSJ International Conference on Intelligent Robots and Systems, pp. 2246–2251, IEEE, 2008.

[2] R. Mahmoud, A. Ueno, and S. Tatsumi, "Dexterous mechanism design for an anthropomorphic artificial hand: Osaka city university hand i," in 2010 10th IEEE-RAS International Conference on Humanoid Robots, pp. 180–185, IEEE, 2010.

[3] M. S. Johannes, J. D. Bigelow, J. M. Burck, S. D. Harshbarger, M. V. Kozlowski, and T. Van Doren, "An overview of the developmental process for the modular prosthetic limb," Johns Hopkins APL Technical Digest, vol. 30, no. 3, pp. 207–216, 2011.

[4] U. Kim, D. Jung, H. Jeong, J. Park, H.-M. Jung, J. Cheong, H. R. Choi, H. Do, and C. Park, "Integrated linkage-driven dexterous anthropomorphic robotic hand," Nature communications, vol. 12, no. 1, pp. 1–13, 2021.

[5] G. P. Kontoudis, M. Liarokapis, K. G. Vamvoudakis, and T. Furukawa, "An adaptive actuation mechanism for anthropomorphic robot hands," Frontiers in Robotics and AI, vol. 6, p. 47, 2019.

[6] E. N. Gama Melo, O. F. Aviles Sanchez, and D. Amaya Hurtado, "Anthropomorphic robotic hands: a review," Ingeniería y desarrollo, vol. 32, no. 2, pp. 279–313, 2014.

[7] B. Zhang, "Design and analysis of a robot hand based on the combination of continuous flexible finger and rigid tendon drive fingers," in Journal of Physics: Conference Series, vol. 1802, p. 022013, IOP Publishing, 2021.

[8] S. R. Kashef, S. Amini, and A. Akbarzadeh, "Robotic hand: A review on linkage-driven finger mechanisms of prosthetic hands and evaluation of the performance criteria," Mechanism and Machine Theory, vol. 145, p. 103677, 2020.

[9] J. R. Napier, "The prehensile movements of the human hand," The Journal of bone and joint surgery. British volume, vol. 38, no. 4, pp. 902–913, 1956.

[10] N. Jarque-Bou, M. Atzori, and H. Müller, "A large calibrated database of hand movements and grasps kinematics," Scientific Data, vol. 7, 01 2020.

[11] C. Systems, CyberGlove II, 2017.

[12] M. Atzori, A. Gijsberts, C. Castellini, B. Caputo, A.-G. M. Hager, S. Elsig, G. Giatsidis, F. Bassetto, and H. Müller, "Electromyography data for non-invasive naturally-controlled robotic hand prostheses," Scientific data, vol. 1, no. 1, pp. 1–13, 2014.

[13] The AnyBody Modeling System (Version 7.3.x) (2022). [Computer software]. Aalborg, Denmark: AnyBody Technology. Available from http://www.anybodytech.com, 2022.

[14] The AnyBody Managed Model Repository (Version 2.3.4) (2022). [Computer software]. Aalborg, Denmark: AnyBody Technology. Available from http://www.anybodytech.com, 2022.

[15] R. J. Palmer, "Polyamides, plastics," Kirk-Othmer Encyclopedia of Chemical Technology, 2000.

[16] L. Tian, N. Magnenat Thalmann, D. Thalmann, and J. Zheng, "The making of a 3d-printed, cable-driven, single-model, lightweight humanoid robotic hand," Frontiers in Robotics and AI, vol. 4, p. 65, 2017.

[17] H. Brorson, C.-O. Werner, and K.-G. Thorngren, "Normal pinch strength," Acta Orthopaedica Scandinavica, vol. 60, no. 1, pp. 66–68, 1989.